"World avoided" simulations with the Whole Atmosphere Community Climate Model

Rolando R. Garcia,[1] Douglas E. Kinnison,[1] and Daniel R. Marsh[1]

Received 3 July 2012; revised 13 September 2012; accepted 19 October 2012; published 13 December 2012.

[1] We use the Whole Atmosphere Community Climate Model, coupled to a deep ocean model, to investigate the impact of continued growth of halogenated ozone depleting substances (ODS) in the absence of the Montreal Protocol. We confirm the previously reported result that the growth of ODS leads to a global collapse of the ozone layer in mid-21st century, with column amounts falling to 100 DU or less at all latitudes. We also show that heterogeneous activation of chlorine in the lower stratosphere hastens this collapse but is not essential to produce it. The growth of ODS, which are also greenhouse gases, produces a radiative forcing of 4 W m^{-2} by 2070, nearly equal that of the non-ODS greenhouse gases CO_2, CH_4, and N_2O in the RCP4.5 scenario of IPCC. This leads to surface warming of over 2 K in the tropics, 6 K in the Arctic, and close to 4 K in Antarctica in 2070 compared to the beginning of the century. We explore the reversibility of these impacts following complete cessation of ODS emissions in the mid-2050s. We find that impacts are reversed on various time scales, depending on the atmospheric lifetime of the ODS that cause them. Thus ozone in the lower stratosphere in the tropics and subtropics recovers very quickly because the ODS that release chlorine and bromine there (e.g., methyl chloroform and methyl bromide) have short atmospheric lifetimes and are removed within a few years. On the other hand, ozone depletion in the polar caps and global radiative forcing depend on longer-lived ODS, such that much of these impacts persist through the end of our simulations in 2070.

Citation: Garcia, R. R., D. E. Kinnison, and D. R. Marsh (2012), "World avoided" simulations with the Whole Atmosphere Community Climate Model, *J. Geophys. Res.*, *117*, D23303, doi:10.1029/2012JD018430.

1. Introduction

[2] Halogenated ozone depleting substances (hereafter, ODS) have been regulated by the Montreal Protocol and its amendments since 1987, following the discovery of the Antarctic ozone hole [*Farman et al.*, 1985] and the identification of the role of chlorine and bromine species in its formation [*Solomon et al.*, 1986; *Molina and Molina*, 1987]. The Protocol has been remarkably successful in controlling the growth of ODS, and it is now known that the stratospheric load of chlorine and bromine compounds is decreasing as expected [e.g., *Anderson et al.*, 2000; *Solomon et al.*, 2006; *Froidevaux et al.*, 2006; *Jones et al.*, 2011]. There is also recent evidence that the control of ODS has led to an increase of ozone in the stratosphere (see, e.g., *Mäder et al.* [2010] and *Salby et al.* [2012], who use linear regression methods to infer that stratospheric ozone began to recover around the turn of the 21st century).

[3] These findings stand in stark contrast to model predictions of the impact of uncontrolled growth of ODS [e.g., *Prather et al.*, 1996; *Morgenstern et al.*, 2008]. Much of this work has been reviewed by *Newman et al.* [2009], who went on to show that growth of ODS at the rate observed in the late 1980s produces a collapse of the global ozone layer. Ozone column amounts fall below 200 Dobson units (DU) by the middle of the 21st century and decrease further to under 100 DU by 2065 at almost all latitudes. Newman et al. performed their calculations using the Goddard Earth Observing System (GEOS5) model, a chemistry-climate model that takes into account feedbacks among ozone photochemistry, radiative heating, and temperature. They found that in the tropical lower stratosphere, a positive feedback loop among temperature, destruction of ozone by heterogeneous reactions favored by low temperatures, and further reduction of temperature due to decreased ozone heating, leads to almost complete removal of ozone after midcentury. Following *Morgenstern et al.* [2008], Newman et al. referred to this scenario of global ozone collapse as the "world avoided" by the adoption of the Montreal Protocol.

[4] In addition to their role in destroying ozone, chlorine and bromine compounds are important greenhouse gases (GHG). This was discussed recently by *Velders et al.* [2007], who estimated the radiative forcing due to ODS in the absence of the Montreal Protocol. Radiative forcing is a commonly used measure of the potential impact of a radiatively active agent (GHG, aerosols, volcanic eruptions, etc.)

[1]National Center for Atmospheric Research, Boulder, Colorado, USA.

Corresponding author: R. R. Garcia, National Center for Atmospheric Research, Boulder, CO 80307-3000, USA. (rgarcia@ucar.edu)

0148-0227/12/2012JD018430

on the global energy budget [see, e.g., *Hansen et al.*, 2005]. It is expressed as the instantaneous radiative flux imbalance ($W\ m^{-2}$) that results from adding a specified burden of GHG to the preindustrial (ca. 1850) atmosphere, which is assumed to be in global radiative balance. The imbalance is often calculated after allowing the atmosphere above the tropopause to adjust, since this takes place on a short time scale and modifies the forcing at tropopause level; we adopt this definition in the estimates of radiative forcing discussed later. Velders et al. showed that, had ODS remained uncontrolled after 1987, the radiative forcing in 2010 would have reached 0.6 $W\ m^{-2}$, which is approximately one third of the radiative forcing attributable to anthropogenic CO_2 in that year. By 2020, the radiative impact of unregulated ODS would reach 0.8–0.9 $W\ m^{-2}$, nearly 40% of that due to CO_2.

[5] While it is clear that the potential climate impact of unregulated ODS growth is important, *Newman et al.* [2009] could not address this question because the GEOS5 model does not take into account the coupling between the atmosphere and the ocean. Tropospheric temperature changes due to GHG increases are strongly conditioned by the response of the ocean and can only be computed consistently with a coupled ocean-atmosphere model. Thus one purpose of the present study is to extend the results of Newman et al. by considering both the photochemical and climatic impacts of uncontrolled ODS growth in the 21st century. To this end, we use the most recent version of the Whole Atmosphere Community Climate Model, coupled to a global ocean model. We investigate the chemical and climatic impacts of ODS growth under the same scenario envisaged by Newman et al., as well as two additional questions: the ultimate role of heterogeneous chemistry in the destruction of ozone in the tropical lower stratosphere, and the reversibility of the effects of ODS following an immediate cessation of emissions in the 2050s.

2. Numerical Model and Scenarios

[6] The Whole Atmosphere Community Climate Model, version 4 (WACCM4) is a "high-top" chemistry-climate model developed at the National Center for Atmospheric Research (NCAR) [*Garcia et al.*, 2007; *Marsh et al.*, 2007; *Tilmes et al.*, 2007]. The model domain extends from the surface to about 140 km of altitude, with horizontal resolution of 2.5° × 1.9° (longitude × latitude), and variable vertical resolution, of about 1.25 km in the troposphere and lower stratosphere, 1.75 km in the upper stratosphere, and 3.5 km in the upper mesosphere and thermosphere.

[7] The chemical module used in WACCM4 is based on the Model of Ozone and Related Tracers, version 3 (MOZART-3), described by *Kinnison et al.* [2007]. The latter includes all species in the O_X, NO_X, HO_X, ClO_X, and BrO_X chemical families, along with CH_4 and its degradation products (a total of 59 species and 217 gas-phase chemical reactions). Rate constants are based on *Sander et al.* [2006]. In addition, there are 17 heterogeneous reactions on three aerosol types: Nitric Acid Trihydrate (NAT), Supercooled Ternary Solution (STS), and Water-Ice (ICE). The heterogeneous chemistry module uses an equilibrium approach to simulate STS, NAT, and ICE aerosols. In WACCM, the primary heterogeneous halogen activation processes occur on STS aerosols. The STS surface area density is derived using composition results taken from the thermodynamic equilibrium model described in *Tabazadeh et al.* [1994]. The reaction probability information for STS aerosol is taken from *Sander et al.* [2006]. STS halogen activation increases rapidly with decreasing temperature below ~195 K. WACCM4 has been compared to other chemistry-climate models and found to perform well in the model evaluation exercise conducted by the Stratospheric Processes and their Relation to Climate (SPARC) project [see *Eyring et al.*, 2010].

[8] WACCM4 does not generate a quasi-biennial oscillation (QBO) spontaneously, but one is imposed by relaxing stratospheric tropical winds to observations [*Matthes et al.*, 2004]. The model includes a parameterization for (unresolved) mesoscale gravity waves, which is triggered by diagnosed convection and frontal systems, in addition to orography [*Richter et al.*, 2010]. WACCM4 is a component of NCAR's Community Earth System Model [*Gent et al.*, 2011] and may be run coupled to a deep ocean model, the Parallel Ocean Processor [*Smith et al.*, 2010]. In this configuration, which we use here, WACCM4 becomes a fully interactive climate model.

[9] For the present investigation, WACCM4 was run between 1985 and 2070 under two principal scenarios:

[10] 1. A reference simulation (CONTROL) that imposes as surface boundary conditions the observed abundances of all relevant GHG through 2005 [*Meinshausen et al.*, 2011a]. After 2005 the non-ODS greenhouse gases, CH_4, N_2O, and CO_2, change according to the 4.5 $W\ m^{-2}$ "stabilization" radiative concentration pathway (RCP4.5) of the Intergovernmental Panel on Climate Change (IPCC) [*van Vuuren et al.*, 2011; *Meinshausen et al.*, 2011a]. In this scenario, GHG produce a radiative forcing of approximately 4.5 $W\ m^{-2}$ in 2100. All ODS of anthropogenic origin are assumed to follow the evolution expected under the Montreal Protocol and its amendments, consistent with scenario A1 of *World Meteorological Organization* [2007], with some modifications, as discussed by *Meinshausen et al.* [2011b]. This simulation serves as a basis of comparison for other scenarios in the 21st century.

[11] 2. A "world avoided" simulation (WAVD), which is identical in all respects to CONTROL, except that ODS are prescribed to grow at a rate of 3.5% per year from 1985 onwards. Chlorine from methyl chloride does not increase in WAVD, as this species has only natural sources. Note that our 3.5% growth rate is somewhat larger than the 3% per year used by *Newman et al.* [2009], who allowed ODS to grow at starting in 1974, almost a decade earlier than in our simulation. The faster growth rate used in WAVD produces approximately the same loading of ODS in the middle to late 21st century as in Newman et al.'s study (about 15–50 ppbv EECL in 2030–2070), such that our results may be compared to theirs during the period of maximum ozone loss. As we shall see, the WAVD scenario leads to a total radiative forcing in the late 21st century of more than 8 $W\ m^{-2}$.

[12] Figure 1 summarizes the evolution of the non-ODS greenhouse gases and of the ODS in the CONTROL and WAVD scenarios. The ODS burden is given in terms of Equivalent Effective Chlorine (EECL) (Figure 1d). EECL is a linear combination of the mixing ratios of the ODS weighted according to their efficiency as catalysts of ozone destruction [see *Newman et al.*, 2009]. The species that make up EECL in WACCM4 are listed on Table 1. In the CONTROL simulation (black curves), CH_4 decreases

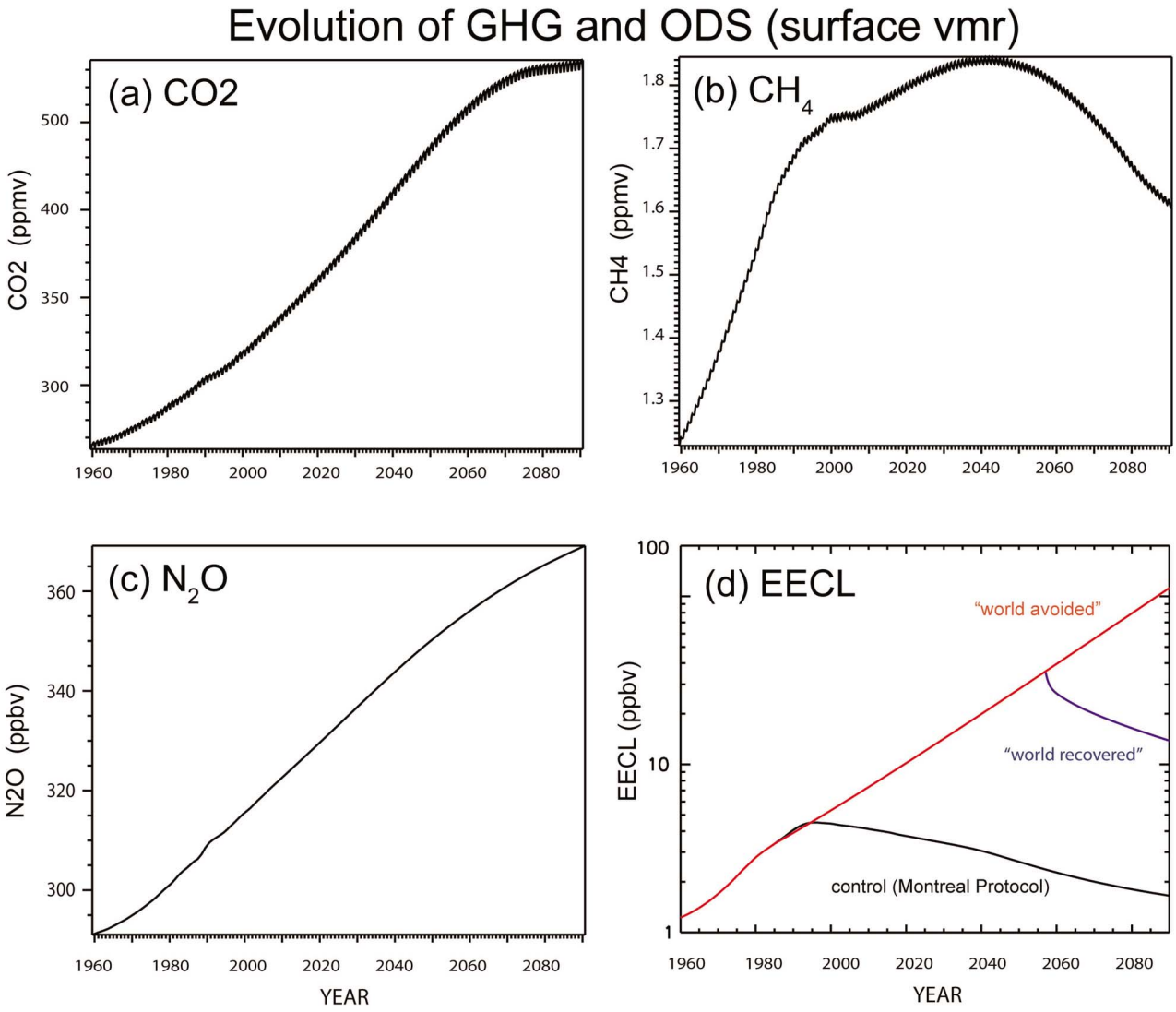

Figure 1. Time series of the mixing ratio boundary conditions for ODS and non-ODS greenhouse gases used in the control and world avoided simulations: (a) CO_2, (b) CH4, and (c) N_2O evolve identically in both simulations, according to scenario RCP4.5 of IPCC. (d) The evolution of ODS in terms of "equivalent effective chlorine" (EECL). In the control case, it decreases after 1987 according to the Montreal Protocol, whereas in the world avoided simulation (red) it continues to increase at 3.5% per year after 1987. Also shown in Figure 1d, in blue, is the evolution of EECL in the "world recovered" case (see text for details).

toward the end of the 21st century, the growth of CO_2 is stabilized, and ODS decrease according to the Montreal Protocol. In WAVD, the evolution of the GHG is identical to CONTROL, but the ODS increase as shown in the red curve for EECL.

[13] In addition to these scenarios, two additional, simulations were made in order to investigate other features of ozone photochemistry and radiative forcing:

[14] 1. A "no-heterogeneous chemistry" simulation (NHET), which is identical in all respects to WAVD except that heterogeneous halogen chemistry is not taken into account in the Tropics. Thus the reaction of ClO with NO_2 is able to sequester chlorine in the reservoir $ClONO_2$. Insofar as *Newman et al.* [2009] documented the importance of heterogeneous chemistry in the collapse of the tropical ozone column, it is interesting to see to what extent this is avoided in the absence of heterogeneous chemistry. Note, however, that the "nonhalogen" heterogeneous reaction of N_2O_5 with H_2O is still included in this simulation. Retaining this reaction keeps NO_X/NO_Y partitioning due to nonhalogen processes consistent with the WAVD simulation.

[15] 2. A "world recovered" simulation (WREC), which follows the WAVD scenario through 2057, at which point emission of ODS are assumed to cease instantly. This is implemented by prescribing a lower boundary condition for each anthropogenic ODS such that its mixing ratio decreases exponentially with an e-folding time equal to its atmospheric lifetime (see Table 1). In the case of methyl bromide, whose

Table 1. Anthropogenic ODS in WACCM4[a]

Species	Chemical Formula	τ/RE	vmr 1987	vmr 2057	vmr 2070
CFC-11	CCl_3F	45/0.25	0.22	2.46	3.88 (1.85)
CFC-12	CCl_2F_2	100/0.32	0.39	4.52	7.12 (3.97)
CFC-113	CCl_2FCClF_2	85/0.3	0.045	0.52	0.83 (0.45)
CFC-114*	$CClF_2CClF_2$				
CFC-115*	$CClFCF_3$				
Carbon tetrachloride	CCl_4	26/0.13	0.1	1.22	1.92 (0.74)
Methyl chloroform	CH_3CCl_3	5/0.06	0.11	1.28	2.02 (0.095)
HCFC-22	$CHClF_2$	12/0.2	0.06	0.70	1.11 (0.24)
HCFC-142b*	CH_3CCl_2F				
Halon-1211	$CBrClF_2$	16/0.3	0.001	0.016	0.024 (0.007)
Halon-2402*	$CBrF_2CBrF_2$				
Methyl bromide	CH_3Br	0.7/0.01	0.009	0.11	0.17 (0.006)
Halon-1202*	CBr_2F_2				
Halon-1301	$CBrF_3$	65/0.32	0.0006	0.0076	0.012 (0.006)

[a]Atmospheric lifetimes (τ, in years) and radiative efficiencies (RE, in W m^{-2} ppbm^{-1}), from *World Meteorological Organization* [2011, Tables 1–3] and *Intergovernmental Panel on Climate Change* [2007, Tables 2–14], respectively. Species marked with an asterisk are not computed explicitly in the model, but their effect is taken into account by adjusting stoichiometrically the mixing ratio of the species listed immediately above them, which has a similar loss rate profile. Species mixing ratios (in ppbv) at three times during the "world avoided" simulation are shown in columns 4–6. The value in parenthesis in the last column is the mixing ratio in 2070 in the "world recovered" case.

abundance has a natural component, the decrease is halted when it reaches the mixing ratio due to natural sources (5.8 pptv). The intent of this simulation is to investigate to what extent the chemical and climatic changes brought about by uncontrolled ODS growth might be reversed if injection into the atmosphere were to cease completely. The evolution of EECL in this simulation is shown by the blue curve in Figure 1d.

[16] The impact of each of these scenarios on stratospheric chemistry and tropospheric warming is discussed in the following sections.

3. Stratospheric Ozone in the World Avoided

[17] The CONTROL and WAVD simulations were run through the year 2070, by which time very large chemical and radiative impacts become evident. We consider first the effect of ODS growth in WAVD on stratospheric ozone. Figure 2 shows the calculated zonal-mean ozone volume mixing ratio as a function of latitude and altitude in November 2070. The color-filled contours denote the results for the CONTROL case, while the superimposed line contours represent ozone under WAVD. The effect of the very large burden of ODS in the world avoided simulation has reduced sharply the ozone abundance everywhere in the stratosphere. This is particularly evident in the upper stratosphere, above 5 hPa, where the ozone mixing ratio in WAVD is about a quarter of the value in the CONTROL case, and in the lowermost stratosphere, below about 40 hPa, where ozone has been practically eliminated at all latitudes (mixing ratios of 0.5 ppmv or smaller). The ozone maximum in the middle stratosphere has been reduced by about a factor of two (5.5 ppmv versus 10.5 ppmv), and its altitude has dropped from the 6 hPa level to near 10 hPa. The downward shift of the ozone maximum is a result of "self-healing," as the very large reduction of ozone in the upper stratosphere allows deeper penetration of ultraviolet (UV) radiation and increases ozone production near 10 hPa.

[18] The loss of stratospheric ozone under WAVD is even more dramatic when considered in terms of the total column, that is, the integrated amount of ozone between the surface and the top of the atmosphere. Figure 3 shows the evolution of the ozone column in the CONTROL and WAVD simulations between 2005 and 2070. The results have been smoothed with a 13-month running mean to remove the seasonal cycle and emphasize secular changes; this is why the seasonal development of a deep Antarctic ozone hole is not apparent in either simulation at the beginning of the century. What is apparent is that the smoothed ozone column at Antarctic latitudes increases to 250–275 DU by 2070 in the CONTROL case as a result of the sharp reduction of ODS (cf. Figure 1); elsewhere we see more modest increases in ozone column, which again are the result of the reduction of ODS by the Montreal Protocol. Indeed, by 2070 the ozone column has recovered to values comparable to or higher than the amounts observed in the 1980s (not shown). On the other hand, in WAVD, the smoothed ozone column continues to

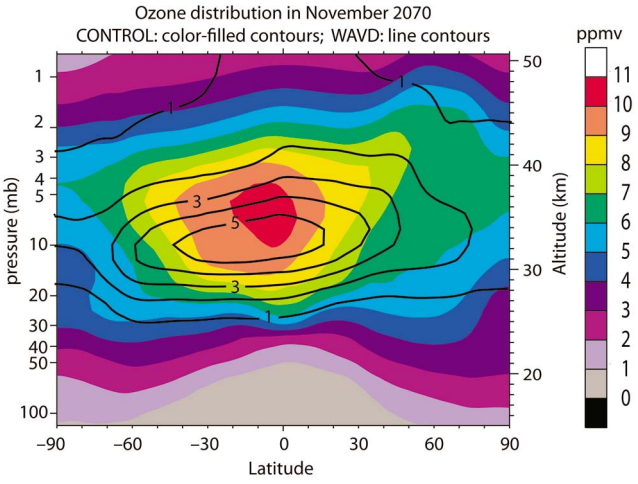

Figure 2. Zonal-mean ozone distributions from the control (color fill) and world avoided (line contours) simulations in November 2070. Severe ozone loss is seen in the world avoided case throughout the stratosphere, and especially below 30–40 hPa, where ozone has been essentially eliminated.

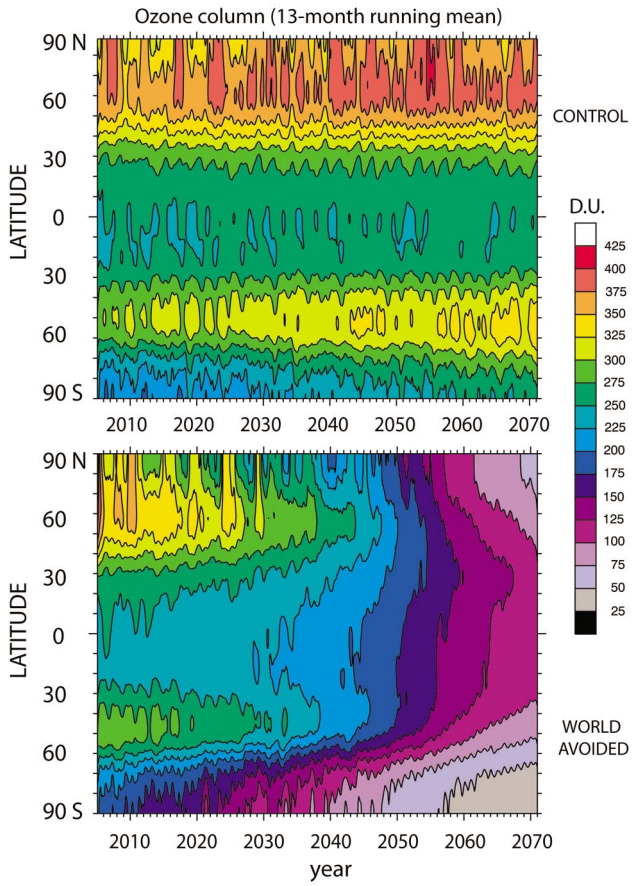

Figure 3. Evolution of the total ozone column (DU) in the (top) control and (bottom) world avoided simulations. The times series have been smoothed with a 13-month running mean to suppress the annual cycle and emphasize secular changes.

decrease over Antarctica, to less than 50 DU in 2070 and, perhaps more remarkably, it decreases to about 100 DU throughout the Tropics and midlatitudes. This is the "global ozone hole" documented in the simulations by *Newman et al.* [2009]. It is reproduced here with a completely independent model with approximately the same magnitude and timing [cf. *Newman et al.*, 2009, Figure 3] which suggests that the collapse of the ozone layer is a robust effect of the greatly increased ODS burden. We note also that, as in Newman et al., the tropical ozone column in WAVD remains relatively stable until the 2040s, at which time it undergoes a precipitous decline, driven by very fast ozone loss in the lower stratosphere. Newman et al. argued that, in their GEOS5 model, the sudden decline of ozone in the lower tropical stratosphere follows decreasing temperatures, which make possible the activation of chlorine by heterogeneous processes. We return to this question in the next section, where the role of heterogeneous chemistry in WACCM4 is discussed in detail.

[19] The impact of the reduced ozone column in WAVD on ultraviolet radiation at the surface, under cloudless skies, is documented in Figure 4, which shows the zonally averaged UV index as a function of latitude in Northern Hemisphere summer for 2000 and 2070. The UV index is a dimensionless measure of UV irradiance in the wavelength band 250–400 nm weighted by its erythemal potential, that is, the ability of UV radiation to produce sunburn in unprotected skin [see, e.g., *World Health Organization* (*WHO*), 2002]. The UV indices shown in Figure 4 are obtained from the ozone profiles calculated under the WAVD scenario, assuming cloudless skies. Under present conditions, the UV index ranges from zero (darkness or very low sunlight) to 12–14 (very strong sunlight in the tropics). A UV index of 11 or higher is considered "extreme" and will quickly cause sunburn in light-skinned individuals. Figure 4 shows that, in 2000, the largest UV index values (~12) occur in the tropics, shifted toward the Northern (summer) Hemisphere, with lowest values (≤2) found in the sunlit high latitudes. In 2070, after the stratospheric ozone layer has collapsed worldwide, the UV index is much larger. Extremely high values, greater than 35, are found in the tropics; the sunlit northern polar cap shows values in the range 5–15, which are comparable to or larger than the values found in the subtropics and tropics in 2000. Such an enhancement of UV irradiance at the surface is beyond anything that modern ecosystems have experienced, and it develops in a very short time, starting in the 2040s. For example, Figure 3 shows that in 2030 column amounts are above 225–250 everywhere north of about 50°S; these values, while low, are experienced today in the tropics. However, by 2060, barely one human generation later, the largest column values anywhere on the globe are less than 150 DU. It thus appears that, if anything like the WAVD scenario were to actually take place, there would be little possibility of adaptation by the global ecosystem.

4. Heterogeneous Chemistry and Ozone Loss in the Lower Stratosphere

[20] We have shown that in the world avoided simulation the ozone column collapses worldwide beginning in the 2040s, and we have noted that the collapse is driven by very

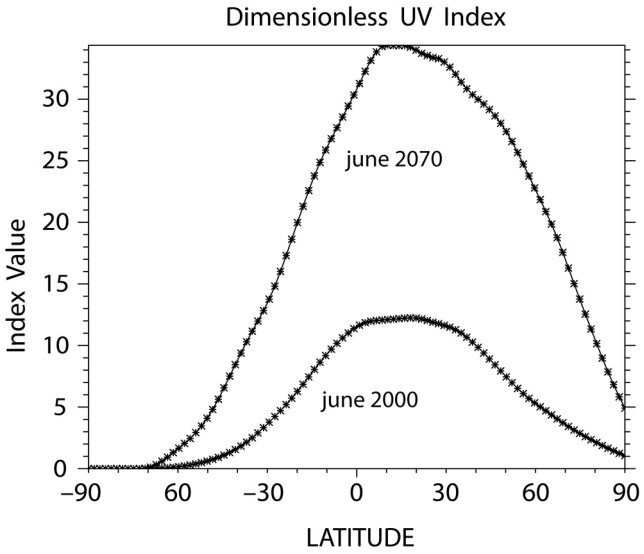

Figure 4. Zonally averaged UV index [*WHO*, 2002] as a function of latitude in June of 2000 and 2070 in the WAVD simulation. Values over 11 are considered "extreme" (see text for details).

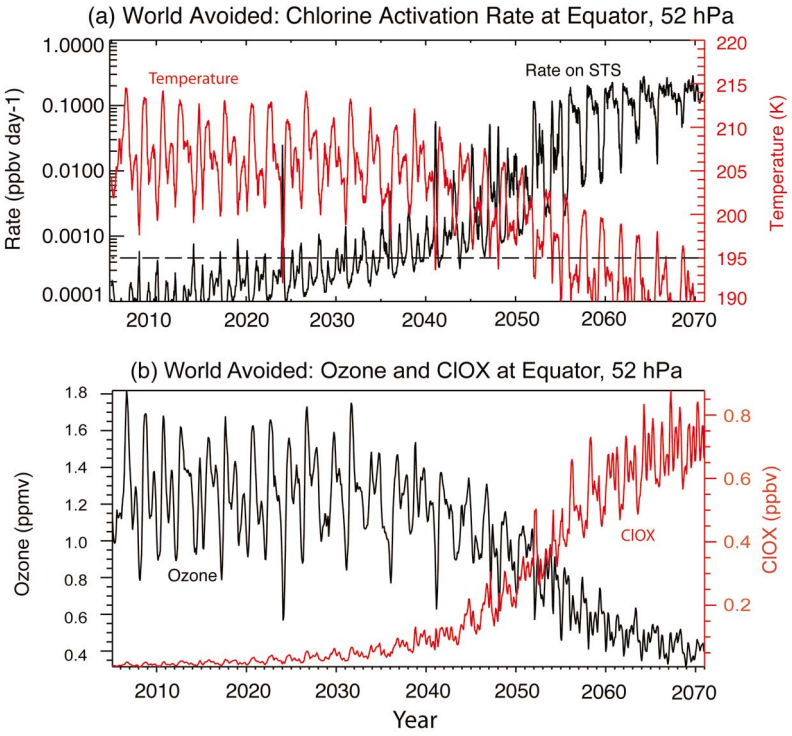

Figure 5. Time series of (a) temperature (K, in red) and activation rate of chlorine (ppbv day^{-1}, black); and (b) ozone (ppmv, black) and active chlorine (ClO_X; ppbv, red) on the Equator at 52 hPa in the world avoided simulation. ClO_X increases and ozone decreases rapidly beginning in the mid-2040s, when chlorine activation becomes frequent. The dashed line in Figure 5a denotes the temperature (195 K) at which heterogeneous chemical processes become important.

rapid ozone removal in the lower stratosphere. *Newman et al.* [2009] discussed the destruction of ozone in the polar lower stratosphere, and everywhere in the middle and upper stratosphere under "world avoided" conditions. Similar processes ("ozone hole" chemistry in the polar regions and gas-phase odd-oxygen catalysis in the middle and upper stratosphere) operate in our calculations, and we do not discuss them further here. We highlight instead the processes that produce the worldwide collapse of the ozone column by focusing on the chemistry of the lower stratosphere in the tropics and evaluating the role of heterogeneous reactions.

[21] Catalytic cycles involving chorine and bromine can play an important role in the ozone balance of the lower stratosphere if a substantial fraction of inorganic chlorine is active chlorine (ClO_X = Cl + 2 Cl_2 + ClO + OClO + 2 Cl_2O_2 + HOCl + BrCl). In particular, the cycle involving the ClO dimer, Cl_2O_2, [*Molina and Molina*, 1987]:

(R1) $$ClO + ClO + M \rightarrow Cl_2O_2 + M$$

(R2) $$Cl_2O_2 + h\nu \rightarrow Cl + ClOO$$

(R3) $$ClOO + M \rightarrow Cl + O_2 + M$$

(R4) $$\frac{2\,(Cl + O_3) \rightarrow 2\,(ClO + O_2)}{2O_3 + h\nu \rightarrow 3\,O_2(\text{net})}$$

and the ClO-BrO cycle:

(R5) $$Cl + O_3 \rightarrow ClO + O_2$$

(R6) $$Br + O_3 \rightarrow BrO + O_2$$

(R7) $$\frac{ClO + BrO \rightarrow Br + Cl + O_2}{2O_3 \rightarrow 3\,O_2(\text{net})}$$

can catalyze ozone destruction efficiently. Both cycles contribute to Antarctic ozone destruction in the present atmosphere, although the dimer cycle is somewhat more important. However, these catalytic cycles can be rendered ineffective if active chlorine is sequestered by reaction of ClO with NO_2, which produces the reservoir species $ClONO_2$. Under present conditions, the destruction of ozone in the lower stratosphere by catalytic cycles involving chlorine and bromine is favored only in Antarctica, where cold temperatures allow the formation of stratospheric clouds. The cloud particles serve as sites for heterogeneous chemical reactions, such as $ClONO_2 + HCl \rightarrow HNO_3 + Cl_2$, which activate chlorine by freeing it from reservoir species.

[22] To highlight the role of chlorine activation in the WAVD scenario, Figure 5a shows equatorial zonal-mean temperature at 52 hPa, together with the activation rate of chlorine on supercooled ternary solutions (see section 2). The short-term variability of the temperature is caused by the

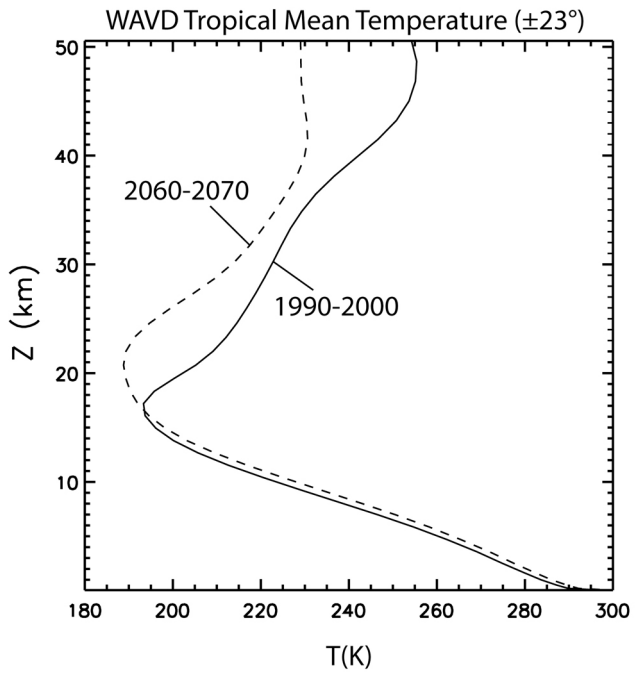

Figure 6. Tropical-mean (±23°) temperature profiles (K) for the world avoided case averaged over 1990–2000 (dashed) and 2060–2070 (solid). Temperatures drop by as much as 20 K in the lower stratosphere and 25 K near the stratopause.

tropical QBO, which is prescribed in WACCM4 (see section 2). Aside from these fluctuations, there is a slow, long-term cooling such that, starting in the 2040s, the temperature approaches and occasionally falls below 195 K during some cold phases of the QBO. As noted in section 2, activation of halogens on STS becomes important around 195 K, and this is reflected in the "spikes" in the rate of chlorine activation that coincide with episodes of low temperature. After 2050, temperatures in the lower stratosphere drop below 195 K for at least part of every year, and the activation rate surpasses 0.1 ppbv of ClO per day, which is typical of activation rates in today's Antarctic ozone hole. Figure 5b shows that ozone begins to decrease rapidly as ClO_X increases.

[23] Ozone loss in turn leads to lower temperatures because of reduced shortwave heating, such that chlorine activation (and further ozone destruction) becomes more efficient. By 2060, equatorial ozone at 52 hPa throughout the tropics and subtropics has fallen below 0.5 ppmv, and annual-mean temperatures colder than 195 K extend from almost 30°N to 30°S in the lower stratosphere. Figure 6 shows tropical-mean vertical profiles of temperature from the WAVD simulation for the decades of 1990–2000 and 2060–2070. The cooling of the lower stratosphere between 20 and 25 km approaches 20 K and the altitude of the tropical tropopause rises from 17 km to about 21 km. Warming of the troposphere appears modest on the scale used to display the stratospheric changes, but it is as much as 4 K in the upper troposphere; this is driven in part by the large radiative forcing introduced by ODS (see section 5). Note also the very large (~25 K) temperature decreases in the upper stratosphere; these are due mainly to the sharp reduction of ozone in that altitude range by gas-phase chemistry, which reduces shortwave heating accordingly.

[24] *Newman et al.* [2009] attributed the cooling of the lower stratosphere during the first few decades of the 21st century, before ozone begins to collapse, to the acceleration of the Brewer-Dobson circulation (BDC) that follows from the effects of increasing GHG. They argued that adiabatic cooling due to stronger tropical upwelling eventually triggers heterogeneous chemistry, which in turn activates chlorine and leads to rapid ozone loss. The acceleration of the BDC under increasing loading of GHG has been widely documented in the literature and is reproduced by many models [e.g., *Butchart et al.*, 2006; *Garcia and Randel*, 2008; *Oman et al.*, 2009; *McLandress and Shepherd*, 2009; *Eyring et al.*, 2010]. It occurs also in our WAVD simulation, where the tropical-mean Transformed Eulerian Mean (TEM) vertical velocity, $\langle w^* \rangle$, increases with time throughout the tropical lower stratosphere (not shown); the magnitude of the tropical-mean linear trend in $\langle w^* \rangle$ near 52 hPa (20 km) between 2005 and 2040 is small, about 0.007 mm s^{-1} per decade, but it is statistically significant at the 95% confidence level.

[25] In order to understand how the secular increase in $\langle w^* \rangle$ influences the temperature of the tropical lower stratosphere, we note that the main contributors to thermodynamic balance in that region are shortwave heating due to absorption by ozone, Q, adiabatic cooling due to tropical upwelling, and infrared relaxation, which we may express as Newtonian cooling, with relaxation coefficient α. It follows from the quasi-steady state thermodynamic equation that secular changes in temperature may be expressed as:

$$\delta T = \frac{1}{\alpha}\left[\delta Q - \delta w^* \left(\frac{HN^2}{R}\right)\right]. \quad (1)$$

With this in mind, we show in Figure 7 the evolution of deseasonalized tropical-mean (±23°) temperature anomalies (with respect to 2005) at 52 hPa in WAVD. The thin black curve represents monthly mean anomalies, while the thick black curve has been smoothed with a 13-month running mean. The temperature decreases slowly between 2005 and about 2040, and much more rapidly thereafter (when widespread chlorine activation and ozone loss begins). Also shown in Figure 7, in red, are curves that represent the adiabatic contribution to the temperature change, the second term on the RHS of equation (1), with $\alpha^{-1} = 50$ days. It can be seen that, before the late 2030s, anomalous cooling is almost entirely explained by enhanced tropical upwelling. On the other hand, after about 2040 the black and red curves diverge rapidly because accelerating ozone loss reduces the shortwave ozone heating, the first term on the RHS of equation (1).

[26] The results shown in Figures 5–7 support the conclusion that chlorine activation by heterogeneous processes triggers the worldwide collapse of the ozone column by creating "Antarctic ozone hole" conditions throughout the tropical lower stratosphere. This raises the question whether such collapse would be less severe in the absence of heterogeneous chemistry; that is, would the almost complete elimination of ozone in the lower stratosphere be averted if chlorine activation did not occur. To investigate this possibility, we carried out a simulation with heterogeneous

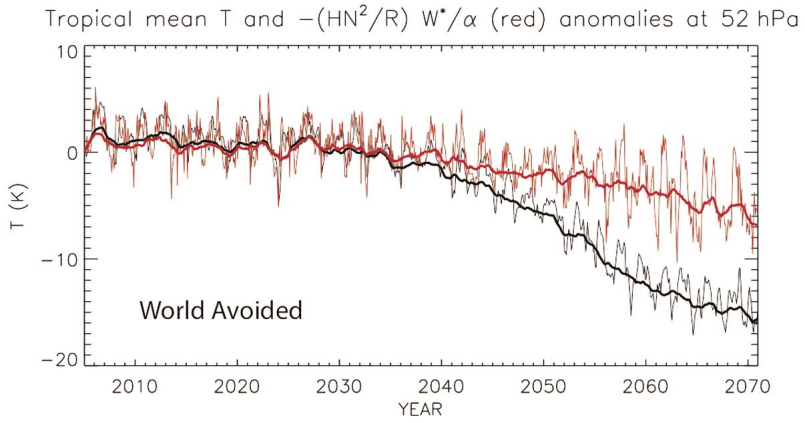

Figure 7. Tropical-mean (±23°) temperature anomalies (with respect to 2005; in K) at 52 hPa in the world avoided simulation. The thin black curve is the monthly mean temperature, while the thick black curve is a 13-month running mean. The red curves represent the contribution of adiabatic cooling to the total temperature anomaly, assuming a thermal relaxation time scale, α^{-1} = 50 days. See text for details.

processing turned off in the model; this is the NHET scenario described in section 2. The results of this simulation are at first glance surprising. The ozone column still collapses worldwide (not shown), and the collapse is due to the almost complete elimination of ozone in the lower stratosphere, just as in WAVD. The main difference with respect to WAVD is that, in the lower stratosphere, rapid ozone loss in NHET occurs 5–10 years later, as shown in Figure 8a; the inception of rapid cooling of the lower stratosphere lags that seen in WAVD by about the same amount (Figure 8b).

[27] This behavior can be understood by comparing the growth of active chlorine, ClO_X, in the lower stratosphere in the WAVD and NHET simulations. Figure 9 shows that, starting in the 2040s, there is more ClO_X in the former than in the latter, and that the difference becomes large in the late 2040s and thereafter, when chlorine activation becomes frequent in WAVD (cf. Figure 5). Nonetheless, by 2060 there is more ClO_X in NHET than there was in WAVD in the early 2050s. Thus the very large load of inorganic chlorine in the lower stratosphere in these scenarios, which exceeds 2 ppbv by 2040 and 5 ppbv by 2050 (not shown), overwhelms the ability of the reaction of ClO with NO_2 to sequester chlorine in $ClONO_2$. Indeed, the abundance of $ClONO_2$ plateaus in the NHET simulation beyond about 2050 (not shown).

[28] An alternative way of understanding the evolution of ozone in these simulations is to consider the balance of terms in the ozone budget of the tropics. The quasi-steady state continuity equation for ozone may be written as [cf. *Tilmes et al.*, 2007]:

$$\frac{O_3}{\tau_d} = \frac{O_3}{\tau_p} - \frac{O_3}{\tau}. \qquad (2)$$

with

$$\tau_d = \left[w^* \frac{d(\ln O_3)}{dz} \right]; \tau_p = (2J_2 O_2)^{-1}; \text{and } \tau_C = (L_3)^{-1}, \qquad (3)$$

where L_3 is the ozone loss rate. The dynamical lifetime, τ_d, is defined here in terms of vertical advection only, since meridional transport is expected to be small in the "tropical

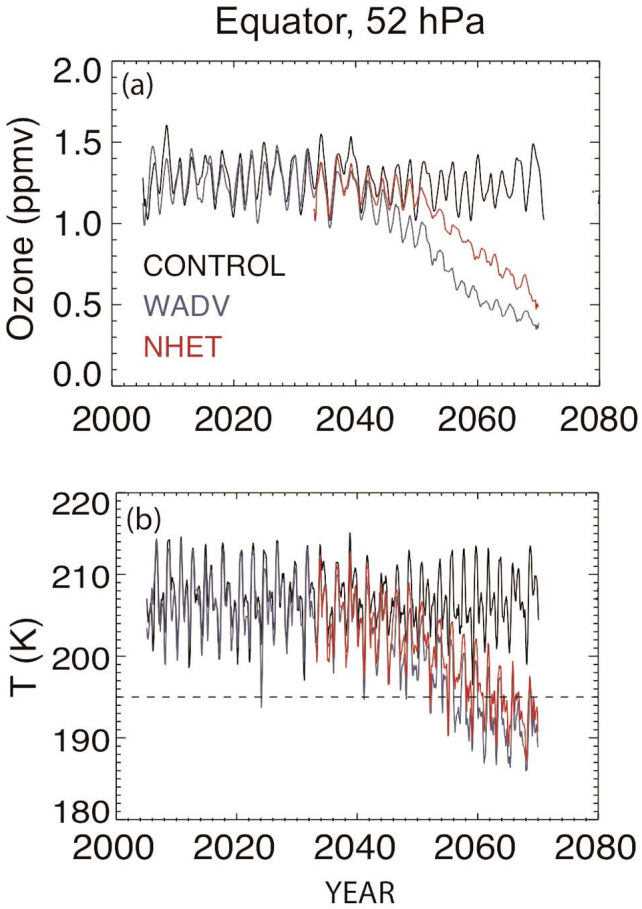

Figure 8. Evolution of (a) zonal-mean ozone (ppmv) and (b) temperature (K) on the Equator at 52 hPa for the control (black), world avoided (WAVD, blue), and world avoided without heterogeneous chemistry (NHET, red) simulations. The dashed line denotes the temperature (195 K) at which heterogeneous chemical processes become important.

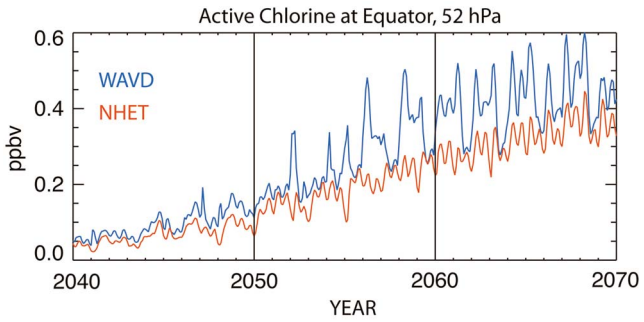

Figure 9. Evolution of active chlorine (ppbv) on the Equator at 52 hPa in the world avoided simulation (WAVD, blue), and in the world avoided simulation without heterogeneous chemistry (NHET, red).

pipe" of the lower stratosphere [*Plumb*, 1996]. We have verified that this is the case in WACCM; that is, we find that equation (2) holds approximately in the model when the effect of dynamics is represented only by mean vertical advection. The production lifetime, τ_p, depends inversely on the photolysis rate of molecular oxygen, J_2, which leads to the formation of ozone. The chemical lifetime, τ_C, includes the contribution of all relevant catalytic families, but it is dominated by the ClO-BrO catalytic cycle, (R5)–(R7), discussed above.

[29] Figure 10 illustrates the behavior of the ozone budget in the WAVD and NHET simulations, in terms of τ_d, τ_p and τ_C at 52 hPa, averaged over ±23° of latitude. The time series have been smoothed with a 13-month running mean to suppress the annual cycle; the remaining short-term variability is, again, due to the influence of the QBO. Before 2030, the ozone budget is dynamically controlled in both simulations; that is, the ozone abundance is set mainly by the equilibrium between dynamics and production, which have time scales of 100–150 days, while the chemical loss time scale is much longer, about 300–500 days. However, τ_C decreases with time and, in WAVD, it drops under 150 days in the mid-2040s and to 30 days by the early 2050s, such that the ozone budget at 52 hPa becomes chemically controlled, with $\tau_C \sim \tau_p$. This is the period when ozone collapses in WAVD, and Figure 10 shows that this happens because of the very rapid decrease of τ_C during that decade. The NHET case follows a similar evolution, the only difference being that the transition to chemical control occurs about 7 years later, in the early 2050s. By 2060 the ozone budget in NHET is also chemically controlled.

[30] These results imply that, given the massive rise in inorganic chlorine in the lower stratosphere in the absence of the Montreal Protocol, heterogeneous chemistry hastens the collapse of the ozone layer but is not necessary to produce it. The chemical loss lifetime in Figure 10 can be seen to decrease from the beginning the 21st century, well before the temperature of the lower stratosphere has become cold enough to activate chlorine by heterogeneous reactions. The onset of chlorine activation produces a very rapid decrease in τ_C during the 2040s, which leads to the collapse of the ozone layer in WAVD. In NHET, continued growth of inorganic chlorine in the lower stratosphere ultimately lowers τ_C sufficiently to collapse the ozone layer a few years later without the need for chlorine activation.

5. Climate Change in the World Avoided

[31] One of the motivations of the present study is to assess the climate impact of very high loads of ODS resulting from growth uncontrolled by the Montreal Protocol. It was noted in section 1 that *Velders et al.* [2007] estimated the radiative forcing due to ODS to be about 0.6 W m^{-2} in 2010. Further uncontrolled growth of ODS in the 21st century increases their global radiative forcing to 4 W m^{-2} by 2070 in our WAVD simulation. This is almost half of the total radiative forcing (by ODS plus CH_4, N_2O, and CO_2) in that year, which is 8.2 W m^{-2}. These estimates were made by calculating the radiative forcing of the additional ODS in 2070 relative to 1850, after allowing for adjustment above the tropopause.

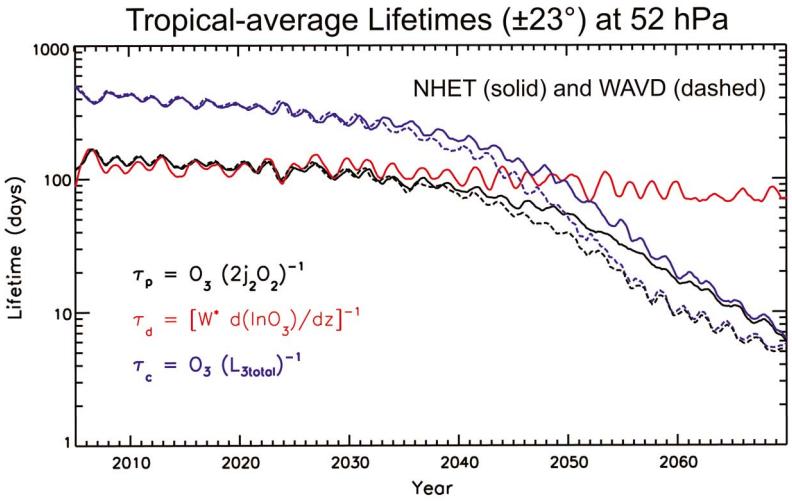

Figure 10. Evolution of the tropical-mean (±23°) chemical production, τ_p (black), dynamical, τ_d (red), and chemical loss, τ_c (blue), lifetimes (days) of ozone at 52 hPa in the world avoided simulation with (WAVD, dashed lines) and without (NHET, solid lines) heterogeneous chemistry.

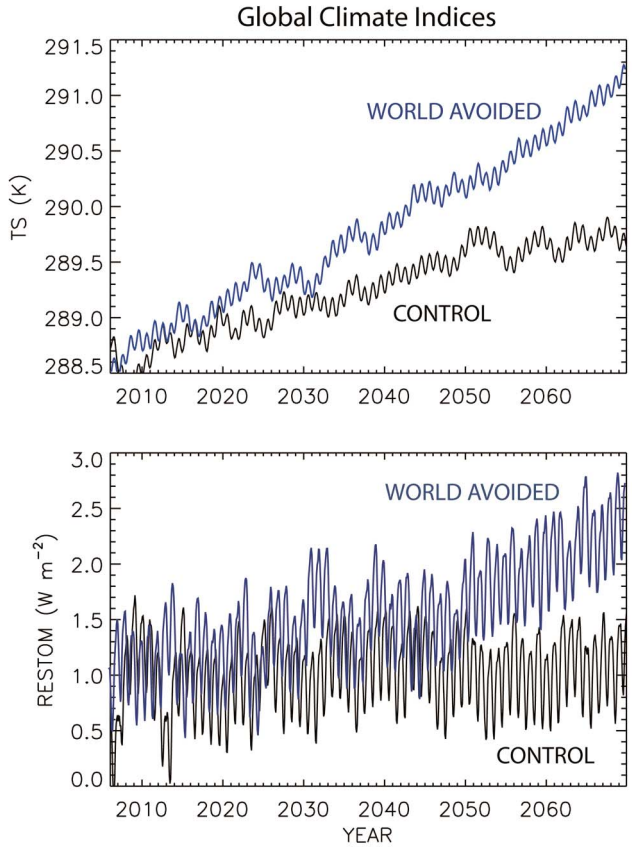

Figure 11. Global-mean indices of climate change in the control (black) and world avoided (blue) simulations. "RESTOM" (W m^{-2}) is the radiative flux imbalance at the top of the model atmosphere; "TS" is the global mean surface temperature (K). The time series have been smoothed with a 25-month running mean to suppress annual and biennial cycles.

[32] Figure 11 shows two globally averaged indicators of climate change: radiative flux imbalance at the top of the model atmosphere (RESTOM) and surface temperature (TS), for the CONTROL and WAVD simulations. In the CONTROL case there is a radiative imbalance of about 1 W m^{-2}, which remains relatively constant throughout the run. Surface temperature rises steadily throughout the period, but the rate of increase begins to slow down after 2050, when CO_2 stabilizes and CH_4 decreases in the RCP4.5 scenario (Figure 1). Between 2005 and 2070 surface temperature increases about 1.5 K, from approximately 288.5 K to a little under 290 K.

[33] In the WAVD simulation, changes in the global-mean climate are much more dramatic. The radiative flux imbalance at the top of the model rises steadily throughout the 21st century, from about 1 W m^{-2} in 2005 to more than 2 W m^{-2} in 2070. Surface temperature also increases continuously, at a faster rate than in the CONTROL case and without any decrease in the rate of growth in the late 21st century. The increase in temperature during the period 2005–2070 is consequently much larger than in the CONTROL case: 2.5 K, from about 288.5 K in 2005 to 291 K in 2070. The marked contrast between the stabilization apparent in the CONTROL simulation and the steady warming in WAVD is of course the result of the growth of ODS in WAVD.

[34] The tropical-mean vertical distribution of temperature changes has already been discussed in the previous section (Figure 6); we note, once again, the substantial warming of the free troposphere, by as much as 4 K, and the increase by about 4 km in the altitude of the tropopause. Longitude versus latitude surface temperature changes between the decadal means for 1990–2000 and 2060–2070 in CONTROL and WAVD are shown in Figure 12, together with the zonally averaged change as a function of latitude. In the CONTROL simulation, there is large (3–5 K), statistically significant warming of the Arctic regions, smaller but statistically significant warming of the tropics (1–2 K), and statistically insignificant changes over much of Antarctica, Eurasia, and North America (Figure 12a). Statistical significance was assessed by a Student's t-test at the 95% confidence level. Zonal-mean temperature changes (Figure 12c, black curve) range from under 1.5 K in the Tropics to 4 K in the Arctic; they are mostly significant except over Antarctica and subpolar latitudes of the Northern Hemisphere, consistent with the patterns of significance in the longitude versus longitude plot. In the WAVD simulation (Figure 12b), the longitude versus latitude pattern of temperature change is similar to that in CONTROL, but strongly magnified. Artic warming exceeds 6 K everywhere, and warming over all land areas, including Antarctica, is now statistically significant; regions of statistically insignificant change are confined to northern Asia and Greenland. Zonal mean changes are roughly double those seen in the CONTROL case, and they are significant at all latitudes (Figure 12c, red curve).

6. Reversibility

[35] The preceding sections have highlighted the large changes in stratospheric chemistry and global climate brought about by increasing ODS in the world avoided scenario. The additional forcing provided by ODS leads to total radiative forcing of over 8 W m^{-2} by 2070, comparable to that in the rising forcing scenario of IPCC, RCP8.5, even though non-ODS greenhouse gases change only at the rate prescribed by the stabilization scenario, RCP4.5. Large as these changes are, their potential impact on the environment and society would appear to be less severe than the calculated changes in stratospheric chemistry, which produce a worldwide collapse of the ozone layer sometime after mid-21st century, even in the simulation (NHET) where heterogeneous chemical processes are ignored.

[36] Sociopolitical responses to slowly developing environmental change are inconsistent, to judge from past and present experience with Antarctic ozone loss and greenhouse warming. Nonetheless, one might suppose that the collapse of the global ozone layer simulated for the mid-21st century in WAVD would elicit a quick societal response, as its consequences would be unarguably catastrophic, and very rapid ozone loss would be evident by 2050. This raises the interesting question whether it is possible to reverse in short order the impacts of the very large load of ODS present in mid-21st century. The question of "reversibility" has been addressed in the context of CO_2-induced warming by, e.g., *Solomon et al.* [2009], who noted that climate change due to

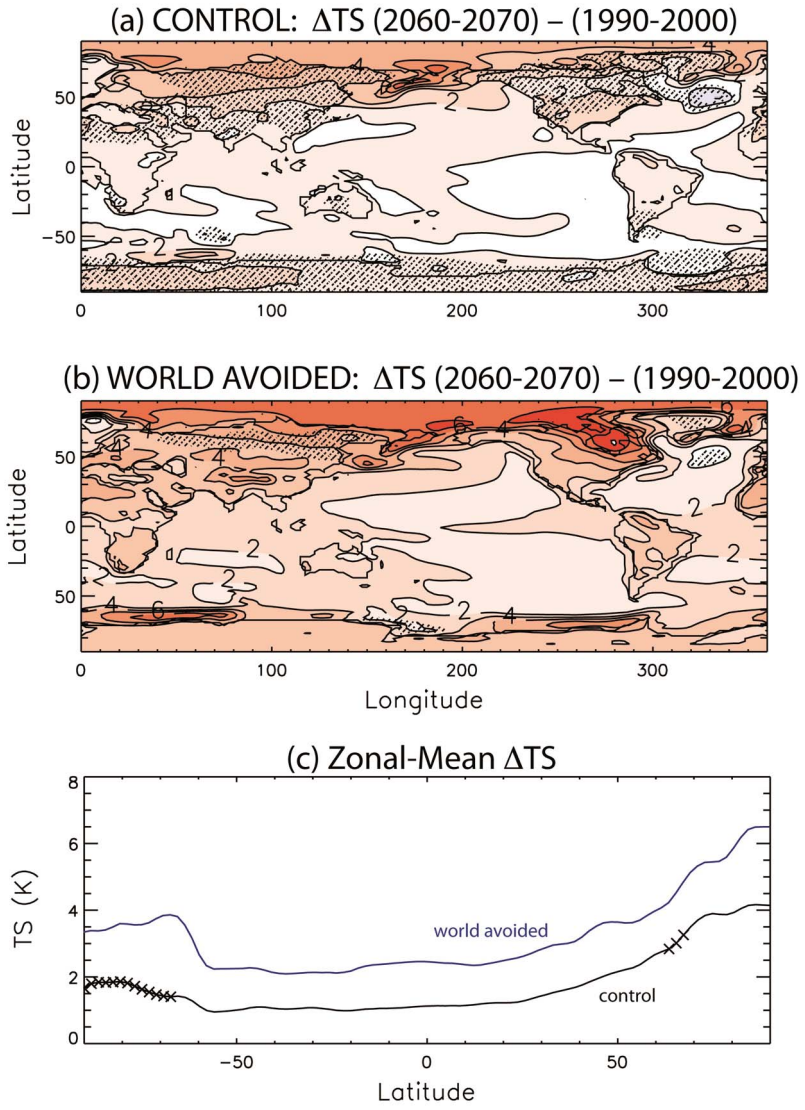

Figure 12. Longitude versus latitude distributions of temperature change (K) between the decades of 1990–2000 and 2060–2070 in the (a) control and (b) world avoided simulations. Changes in the stippled regions are not significant at the 95% confidence level. (c) Zonal-mean temperature changes as functions of latitude, where the crosses denote changes not significant at the 95% level.

increases in CO_2 is essentially irreversible on millennial timescales, even after a total cessation of emissions. This very long time scale is peculiar to CO_2 because of the very long residence time of this gas in the earth system. ODS, on the other hand, have much shorter lifetimes, from about one year (e.g., methyl bromide) to several decades (e.g., CFC-11, CFC-12), as shown in Table 1. Thus we expect their impacts on climate and chemistry to be reversible on a time scale of no more than a century. Of course, insofar as increasing ODS lead to the rapid collapse of the ozone layer shown in Figure 3, reversing this effect over a period of decades would not avert severe environmental damage.

[37] We investigated the recovery of the atmosphere from the effects of ODS growth by conducting a "world recovered" simulation, WREC, wherein all emission of ODS are assumed to cease completely in 2057. Since our model does not prescribe emissions, this is modeled by decreasing the surface mixing ratio of the ODS as explained in section 2. Figure 13 shows the response of the lower equatorial stratosphere to this scenario. Remarkably, ozone and temperature recover to values comparable to those of the CONTROL simulation by 2062, only 5 years after emissions of ODS stop. This happens because ozone destruction in WAVD is dominated by the ClO-BrO cycle (R5)–(R7), and BrO in the tropical lower stratosphere is derived mainly from methyl bromide, which has a very short atmospheric; therefore inorganic Br disappears quickly after emissions cease. This may be seen in Table 1, which shows that the abundance of methyl bromide decreases from 0.11 ppbv in 2057, when ODS emissions cease in WREC, to 0.006 ppbv in 2070 (more than a factor of 10). The effect on the chemical lifetime of ozone is illustrated in Figure 14, which shows the evolution of the total chemical lifetime, τ_C, as well as the partial lifetimes due to chlorine-only and ClO-BrO reactions, denoted

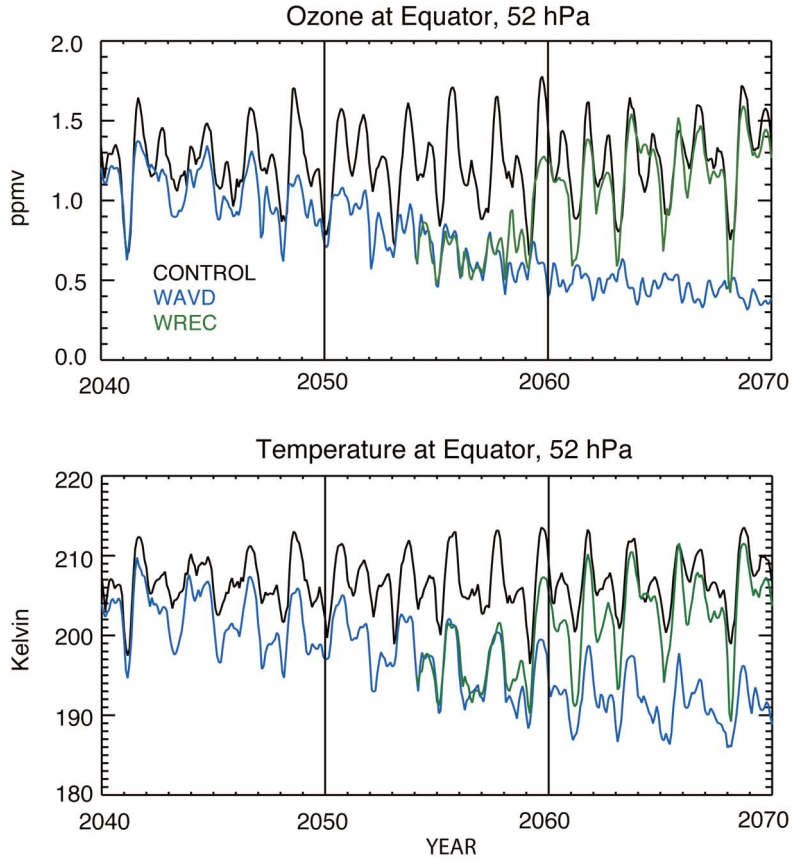

Figure 13. Time series of zonal-mean ozone (ppmv) and temperature (K) on the equator at 52 hPa for the control (black), world avoided (WAVD, blue), and world recovered (WREC, green) simulations. In WREC, emissions of ODS cease completely in 2057; ozone and temperature recover to values comparable to the control case by about 2062.

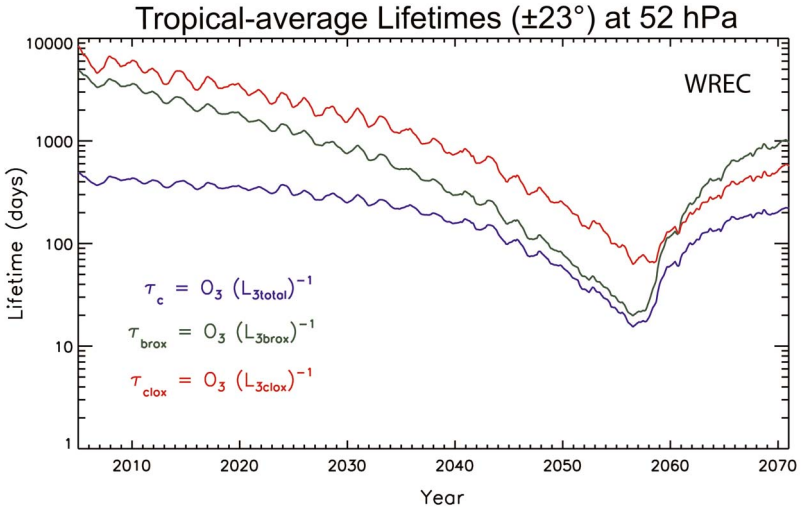

Figure 14. Evolution of the tropical-mean (±23°) chemical lifetime of ozone at 52 hPa in the world recovered simulation. The total chemical lifetime is shown in blue, while the lifetimes due to chlorine-only and chlorine-bromine catalytic cycles are shown in red and green, respectively. See text for details.

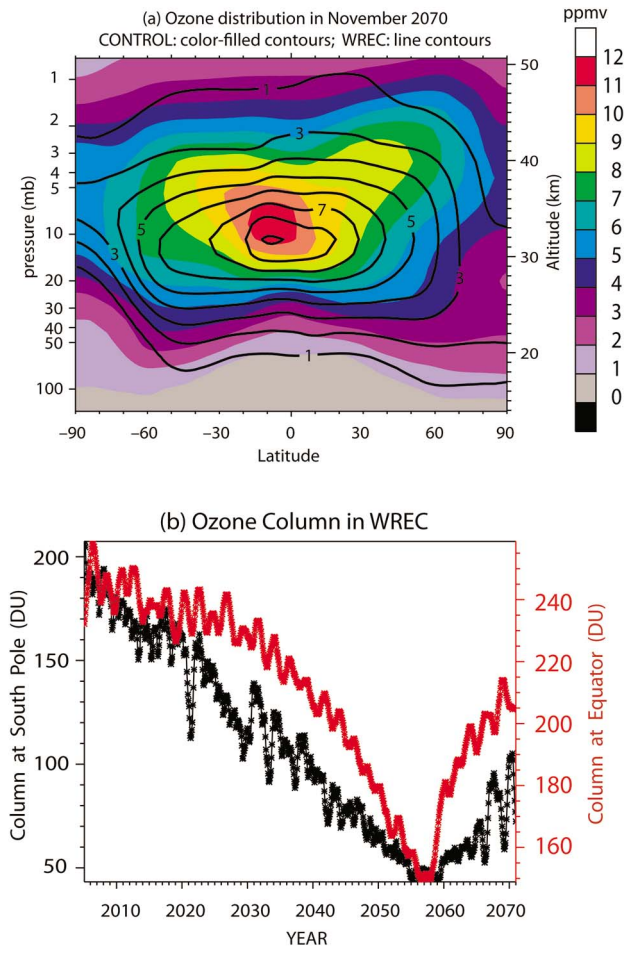

Figure 15. (a) Latitude versus altitude distribution of zonal-mean ozone (ppmv) in November 2070 in the control (color fill) and word recovered (WREC, line contours) simulations. Ozone in WREC has returned to almost normal values in the lower stratosphere outside of the polar regions. (b) Evolution of the ozone column at the Equator (red) and the South Pole (black).

by τ_{ClOx} and τ_{BrOx}, respectively. Catalytic destruction of ozone by the ClO-BrO cycle dominates the loss rate of ozone in the lower stratosphere, with τ_{BrOx} = 20 days in 2057. However, this is quickly reversed once emissions stop, such that τ_{BrOx} increases to over 300 days by 2062 and 1000 days by 2070. Even 300 days is considerably longer than the lifetime due to mean vertical advection (cf. Figure 10); thus ozone is no longer chemically controlled by 2062, consistent with the rapid recovery shown in Figure 13.

[38] The chemical lifetime due to chlorine-only reactions, τ_{ClOx}, is 70–80 days in 2057 (Figure 14, red curve). While much longer than τ_{BrOx}, this would still be fast enough to destroy ozone in the lower stratosphere after the mid-2050s, but τ_{ClOx} also increases rapidly after 2057 to about 500 days in 2070. The reason is that total inorganic chlorine, ClO_Y, decreases relatively rapidly once emissions of ODS stop. In the lower tropical stratosphere, ClO_Y is derived mainly from CFC-11, methyl chloroform, and CCl_4 in roughly equal parts. (The most abundant ODS, CFC-12, contributes relatively little ClO_Y because it is not readily photolyzed in the lower stratosphere; its atmospheric lifetime is 100 years.) While CFC-11 also has a relatively long atmospheric lifetime (45 years), CCl_4 and especially methyl chloroform are considerably shorter lived (26 and 5 years, respectively), such that these species decline sharply between 2057 and 2070, as shown in Table 1. Therefore the total burden of ClO_Y in the lower stratosphere decreases fairly quickly once emissions of ODS cease, from about 4.5 ppbv in 2057 to about 2 ppbv by 2070 (not shown). The chemical loss rate is inversely proportional to the abundance of chlorine, which explains the nearly fivefold decrease in τ_{ClOx} seen in Figure 14.

[39] The results shown in Figures 13–14 indicate that catastrophic ozone loss in the lower stratosphere, outside high latitudes, is quickly reversible because it depends on inorganic chlorine and bromine derived from short-lived species. (Note that the middle latitudes receive air directly from the tropics in the lower stratosphere, such that chemical composition in the former is strongly influenced by that in the latter.) However, this is not the case at high latitudes because the air in those regions is lofted into the middle and upper stratosphere before descending in the polar regions. This provides ample time and exposure to energetic radiation to dissociate the longer-lived ODS. Since the latter have lifetimes of many decades, large ozone losses persist at high latitudes in WREC. This can be seen clearly in Figure 15a, which compares zonal-mean ozone distributions at the end of 2070 for the CONTROL and WREC simulations. Note how, in the tropics and midlatitudes, the ozone mixing ratio below 40–50 hPa (~20–22 km) in WREC is comparable to that found in the CONTROL case, and much higher than in WAVD (cf. Figure 2). However, severe ozone loss remains at higher latitudes, especially over the polar caps. Elsewhere, ozone loss in WREC compared to CONTROL increases with altitude because the ClO_X and BrO_X responsible for this loss is increasingly derived from the longer-lived ODS, which have not been substantially reduced by 2070. For example, Table 1 shows that CFC-12 has decreased only slightly, from 4.52 ppbv in 2057 to 3.97 ppbv in 2070.

[40] The difference in behavior in the tropical versus polar lower stratosphere has an impact on the ozone column, as the latter is dominated by ozone content at the lower altitudes. This is illustrated in Figure 15b, which shows the recovery of the ozone column (smoothed with a 13-month running mean) at the Equator and the South Pole in WREC. In Antarctica, column amounts oscillate between about 60 and 100 DU after 2057. The smaller values are not much larger than the amount in 2057 (50 DU), while the larger values are the result of transport from lower latitudes, where ozone has recovered quickly. For example, at 50°S the ozone column increases from less than 120 DU in 2057 to almost 220 DU in 2070 (not shown). At the Equator, on the other hand, the column has recovered from about 150 DU in 2057 to 200–215 DU by the end of the simulation in 2070.

[41] Another consequence of the slow decrease of the longer-lived ODS is that their impact on climate is also long-lived. Vertical profiles of tropical-mean temperature for the decade of 2060–2070 in WREC and WAVD are compared in Figure 16a. In WREC, temperature in the lowermost stratosphere, especially below ~22 km, has recovered substantially, consistent with the recovery of ozone in this region, and the altitude of the tropopause has decreased from 21 km to about 18 km. On the other hand, cooling in the

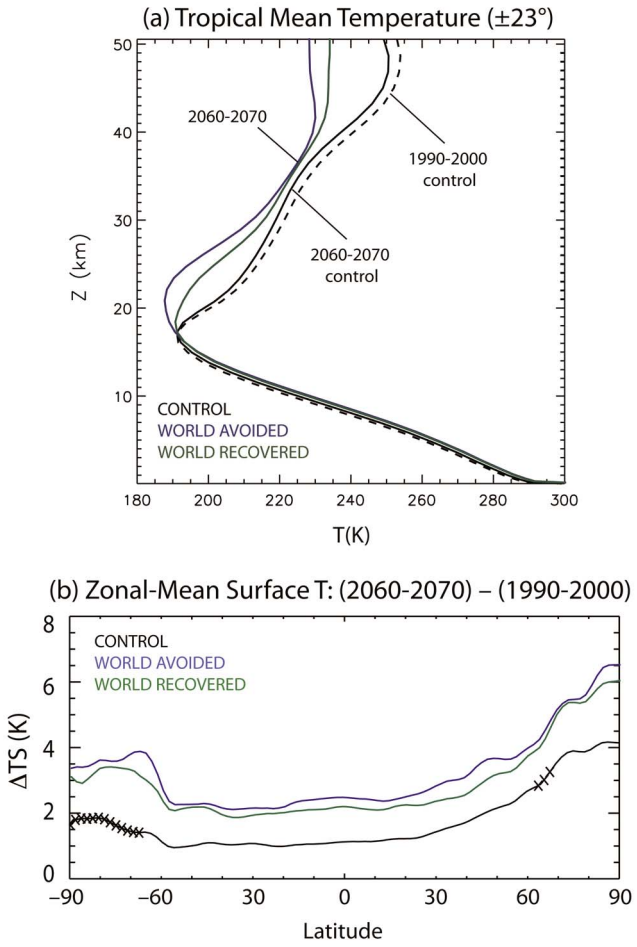

Figure 16. Comparison of (a) tropical-average temperature profiles for the decade of 2060–2070 and (b) zonal-mean surface warming between the decades of 1990–2000 and 2060–2070 in three simulations: control (black), world avoided (blue), and world recovered (green). The dashed curve in Figure 16a is the temperature profile for 1990–200 in the control case, which is very similar to its counterparts in world avoided and world recovered, since ODS have not yet grown appreciably at this time. In Figure 16b the crosses denote changes not significant at the 95% level.

upper stratosphere is almost as large in WREC as in WAVD. Tropospheric temperature change is remarkably similar in WREC and WAVD, such that surface warming is much larger in both of these simulations than in the CONTROL case. In fact, the longitude versus latitude distribution of surface temperature in WREC (not shown) is very similar to that in WAVD (Figure 12). The zonally averaged change in surface temperature as a function of latitude is shown in Figure 16a, where it is compared to the corresponding curves for CONTROL and WAVD. The changes in WREC are almost as large as in WAVD and, as in the latter, they are significant at all latitudes. This is due in part to the fact that the concentration of the long-lived ODS, which also have the largest radiative efficiencies has not decreased much between the time emissions cease, in 2057, and the end of the simulation in 2070 (see Table 1). However, it must be borne in mind that tropospheric temperature change is strongly conditioned by the behavior of the ocean, so the similarity in surface temperature response between WREC and WAVD is also influenced by the thermal inertia of the ocean.

7. Summary and Conclusions

[42] We have used the Whole Atmosphere Community Climate Model to conduct simulations of the "world avoided" by the adoption of the Montreal Protocol. WACCM is a chemistry-climate model that for this investigation is run fully coupled to a deep ocean. When ODS are allowed to continue increasing into the 21st century at the rate (~3.5% per year) they were growing before the adoption of the Protocol, we confirm the finding of *Newman et al.* [2009] that the ozone layer collapses worldwide in the 2040s. Our results are also consistent with a recent, similar study by *Egorova et al.* [2012]. However, an additional simulation where heterogeneous chemical reactions are suppressed shows that these processes are not essential to produce the collapse, although they hasten it by 5–10 years. The load of inorganic chlorine becomes so large by mid-21st century (nearly 5 ppbv) that ozone loss in the lower stratosphere is still very fast despite the sequestration of a substantial fraction of this chlorine in $ClONO_2$. The collapse of the ozone layer takes place very quickly; in the Tropics and subtropics, column amounts decrease from more than 200 DU in 2040 to about 100 DU in 2070. There would be little possibility of adaptation by the global ecosystem to such a rapid change.

[43] The large loading of ODS in the world avoided also has a major impact on tropospheric climate. By 2070, ODS provide almost as much radiative forcing (about 4 W m^{-2}) relative to pre-industrial conditions as the remainder of the GHG included in the world avoided simulation (CO_2, CH_4 and N_2O), which are assumed to grow according to the RCP4.5 scenario of IPCC and produce a radiative forcing of 4.2 W m^{-2} in 2070. Global surface temperature increases by about 2.5 K between 2005 and 2070, to over 291 K. Zonal-mean warming is statistically significant everywhere on the globe, and local warming almost everywhere. Both the northern and southern polar caps warm considerably, with temperature increases of 4–6 K in the Arctic and over 2 K in Antarctica. The deep Tropics warm by 1–2 K, even over the oceans, and the interior of the continents by 2–4 K.

[44] Given the severity of the chemical and climate impacts of uncontrolled growth of ODS, we also investigated the degree to which the changes are reversible if emissions of ODS ceased in the 2050s, a time when the ozone column is collapsing and climate is warming rapidly. While ODS do not have the extremely long atmospheric lifetime of CO_2, some of them (e.g., CFC-12) have lifetimes that approach a century. Nevertheless, in a "world recovered" simulation, wherein emissions of ODS cease abruptly in 2057, ozone in the lower stratosphere recovers completely in about 5 years, except at high latitudes. The reason is that the anthropogenic sources of chlorine and bromine species that destroy ozone in the lower stratosphere, outside the polar caps, are ODS that are readily dissociated at low altitudes and therefore have short atmospheric lifetimes. Once emissions of these ODS cease, the loading of inorganic chlorine and bromine falls rapidly, allowing ozone to recover. However, ozone abundance remains low over the

polar caps because halogen species there are derived from long-lived ODS. The air that reaches the polar lower stratosphere has traveled into the middle and upper stratosphere before descending at high latitudes, which allows sufficient time and exposure to energetic radiation to dissociate these ODS. Thus, the supply of inorganic chlorine and bromine species to the polar lower stratosphere decreases only slowly and ozone depletion persists into the late 21st century. Finally, the climate effects of ODS are also long-lived because they depend on the atmospheric abundance of long-lived species. Tropical mean temperatures warm substantially in the lower stratosphere, where ozone recovery is substantial, but remain cold in the upper stratosphere, where ozone loss is still large. At the surface, the temperature difference between the decades of 1990–2000 and 2060–2070 is almost as large in the world recovered as it is in the world avoided.

[45] The results presented here underscore once again the importance of the Montreal Protocol for the preservation of the stratospheric ozone layer, and they quantify the degree of climate change avoided by the regulation of ODS. While the most severe effect of uncontrolled growth of ODS (the global collapse of the ozone layer) is quickly reversible once emission of ODS ceases, other important effects (polar ozone loss and tropospheric warming) persist for decades.

[46] **Acknowledgments.** We thank Julia Lee Taylor for the calculation of UV indices shown in Figure 4, Andrew Conley for providing estimates of radiative forcing, and J.-F. Lamarque and W. Randel for reviews of the original manuscript. The National Center for Atmospheric Research (NCAR) is sponsored by the U.S. National Science Foundation. The Community Earth System Model (CESM) is supported by the National Science Foundation (NSF) and the Office of Science of the U.S. Department of Energy. Computing resources were provided by NCAR's Climate Simulation Laboratory, sponsored by NSF and other agencies. This research was enabled by the computational and storage resources of NCAR's Computational and Information Systems Laboratory (CISL).

References

Anderson, J., J. M. Russell, and S. Solomon (2000), Halogen Occultation Experiment confirmation of stratospheric chlorine decreases in accordance with the Montreal Protocol, *J. Geophys. Res.*, *105*, 4483–4490, doi:10.1029/1999JD901075.

Butchart, N., et al. (2006), Simulations of anthropogenic change in the strength of the Brewer–Dobson circulation, *Clim. Dyn.*, *27*, 727–741, doi:10.1007/s00382-006-0162-4.

Egorova, T., E. Rozanov, J. Gröbner, M. Hauser, and W. Schmutz (2012), Montreal Protocol benefits simulated with CCM SOCOL, *Atmos. Chem. Phys. Discuss.*, *12*, 17,001–17,030, doi:10.5194/acpd-12-17001-2012.

Eyring, V., T. G. Shepherd, and D. W. Waugh (Eds.) (2010), Chemistry Climate Model Validation, *SPARC Rep. 5*, World Climate Res. Prog., Zurich. (Available from http://www.sparc-climate.org/publications/sparc-reports/).

Farman, J. C., B. G. Gardiner, and J. D. Shanklin (1985), Large losses of total ozone in Antarctica reveal ClO_X/NO_X interaction, *Nature*, *315*, 207–210, doi:10.1038/315207a0.

Froidevaux, L., et al. (2006), Temporal decrease in upper atmospheric chlorine, *Geophys. Res. Lett.*, *33*, L23812, doi:10.1029/2006GL027600.

Garcia, R. R., and W. J. Randel (2008), Acceleration of the Brewer–Dobson Circulation due to increases in greenhouse gases, *J. Atmos. Sci.*, *65*, 2731–2739, doi:10.1175/2008JAS2712.1.

Garcia, R. R., D. Marsh, D. E. Kinnison, B. Boville, and F. Sassi (2007), Simulations of secular trends in the middle atmosphere, 1950–2003, *J. Geophys. Res.*, *112*, D09301, doi:10.1029/2006JD007485.

Gent, P. R., et al. (2011), The Community Climate System Model, version 4, *J. Climate*, *24*, 4973–4991, doi:10.1175/2011JCLI4083.1.

Hansen, J., et al. (2005), Efficacy of climate forcings, *J. Geophys. Res.*, *110*, D18104, doi:10.1029/2005JD005776.

Intergovernmental Panel on Climate Change (2007), *Climate Change 2007: The Physical Science Basis. Contribution of Working Group I to the Fourth Assessment Report of the Intergovernmental Panel on Climate Change*, edited by S. Solomon et al., Cambridge Univ. Press, New York.

Jones, A., J. Urban, D. P. Murtagh, C. Sanchez, K. A. Walker, N. J. Livesey, L. Froidevaux, and M. L. Santee (2011), Analysis of HCl and ClO time series in the upper stratosphere using satellite data sets, *Atmos. Chem. Phys.*, *11*, 5321–5333, doi:10.5194/acp-11-5321-2011.

Kinnison, D. E., et al. (2007), Sensitivity of chemical tracers to meteorological parameters in the MOZART-3 chemical transport model, *J. Geophys. Res.*, *112*, D20302, doi:10.1029/2006JD007879.

Mäder, J. A., J. Staehelin, T. Peter, D. Brunner, H. E. Rieder, and W. A. Stahel (2010), Evidence for the effectiveness of the Montreal Protocol to protect the ozone layer, *Atmos. Chem. Phys.*, *10*, 12,161–12,171, doi:10.5194/acp-10-12161-2010.

Marsh, D. R., R. R. Garcia, D. E. Kinnison, B. A. Boville, S. Walters, K. Matthes, and S. C. Solomon (2007), Modeling the whole atmosphere response to solar cycle changes in radiative and geomagnetic forcing, *J. Geophys. Res.*, *112*, D23306, doi:10.1029/2006JD008306.

Matthes, K., U. Langematz, L. L. Gray, K. Kodera, and K. Labitzke (2004), Improved 11-year solar signal in the Freie Universität Berlin Climate Middle Atmosphere Model (FUB-CMAM), *J. Geophys. Res.*, *109*, D06101, doi:10.1029/2003JD004012.

McLandress, C., and T. G. Shepherd (2009), Simulated anthropogenic changes in the Brewer–Dobson Circulation, including its extension to high latitudes, *J. Clim.*, *22*, 1516–1540, doi:10.1175/2008JCLI2679.1.

Meinshausen, M., et al. (2011a), The RCP greenhouse gas concentrations and their extensions from 1765 to 2300, *Clim. Change*, *109*, 213–241, doi:10.1007/s10584-011-0156-z.

Meinshausen, M., S. C. B. Raper, and T. M. L. Wigley (2011b), Emulating coupled atmosphere-ocean and carbon cycle models with a simpler model, MAGIC6-Part 1: Model description and calibration, *Atmos. Chem. Phys.*, *11*, 1417–1456, doi:10.5194/acp-11-1417-2011.

Molina, L. T., and M. J. Molina (1987), Production of chlorine oxide (Cl_2O_2) from the self-reaction of the chlorine oxide (ClO) radical, *J. Phys. Chem.*, *91*(2), 433–436, doi:10.1021/j100286a035.

Morgenstern, O., P. Braesicke, M. M. Hurwitz, F. M. O'Connor, A. C. Bushnell, C. E. Johnson, and J. A. Pyle (2008), The World Avoided by the Montreal Protocol, *Geophys. Res. Lett.*, *35*, L16811, doi:10.1029/2008GL034590.

Newman, P. A., et al. (2009), What would have happened to the ozone layer if chlorofluorocarbons (CFCs) had not been regulated?, *Atmos. Chem. Phys.*, *9*, 2113–2128, doi:10.5194/acp-9-2113-2009.

Oman, L., D. W. Waugh, S. Pawson, R. S. Stolarski, and P. A. Newman (2009), On the influence of anthropogenic forcings on changes in the stratospheric mean age, *J. Geophys. Res.*, *114*, D03105, doi:10.1029/2008JD010378.

Plumb, R. A. (1996), A "tropical pipe" model of stratospheric transport, *J. Geophys. Res.*, *101*, 3957–3972, doi:10.1029/95JD03002.

Prather, M., P. Midgley, F. S. Rowland, and R. Stolarski (1996), The ozone layer: The road not taken, *Nature*, *381*, 551–554, doi:10.1038/381551a0.

Richter, J. H., F. Sassi, and R. R. Garcia (2010), Toward a physically based gravity wave source parameterization in a General Circulation Model, *J. Atmos. Sci.*, *67*, 136–156, doi:10.1175/2009JAS3112.1.

Salby, M. L., E. A. Titova, and L. Deschamps (2012), Changes of the Antarctic ozone hoe: Controlling mechanisms, seasonal predictability, and evolution, *J. Geophys. Res.*, *117*, D10111, doi:10.1029/2011JD016285.

Sander, S. P., et al. (2006), Chemical kinetics and photochemical data for use in atmospheric studies, *Eval. 15, Publ. 06–2*, Jet Propul. Lab., Pasadena, Calif.

Smith, R. D., et al. (2010), The Parallel Ocean Program (POP) reference manual, Tech. Rep. LAUR-10–01853, Los Alamos Natl. Lab., Los Alamos, N. M.

Solomon, S., R. R. Garcia, F. S. S. Rowland, and D. J. Wuebbles (1986), On the depletion of Antarctic ozone, *Nature*, *321*, 755–758, doi:10.1038/321755a0.

Solomon, P., J. Barrett, T. Mooney, B. Connor, A. Parrish, and D. E. Siskind (2006), Rise and decline of active chlorine in the stratosphere, *Geophys. Res. Lett.*, *33*, L18807, doi:10.1029/2006GL027029.

Solomon, S., G.-K. Plattner, R. Knutti, and P. Friedlingstein (2009), Irreversible climate change due to carbon dioxide emissions, *Proc. Natl. Acad. Sci. U. S. A.*, *106*, 1704–1709, doi:10.1073/pnas.0812721106.

Tabazadeh, A., R. P. Turco, and M. Z. Jacobson (1994), A model for studying the composition and chemical effects of stratospheric aerosols, *J. Geophys. Res.*, *99*(D6), 12,897–12,914, doi:10.1029/94JD00820.

Tilmes, S., D. E. Kinnison, R. R. Garcia, R. Müller, F. Sassi, D. R. Marsh, and B. A. Boville (2007), Evaluation of heterogeneous processes in the polar lower stratosphere in the Whole Atmosphere Community Climate Model, *J. Geophys. Res.*, *112*, D24301, doi:10.1029/2006JD008334.

van Vuuren, D. P., et al. (2011), The representative concentration pathways: An overview, *Clim. Change*, *109*, 5–31, doi:10.1007/s10584-011-0148-z.

Velders, G. J. M., S. O. Andersen, J. S. Daniel, D. W. Fahey, and M. McFarland (2007), The importance of the Montreal Protocol in

protecting climate, *Proc. Natl. Acad. Sci. U. S. A.*, *104*, 4814–4819, doi:10.1073/pnas.0610328104.
World Health Organization (2002), Global solar UV index: A practical guide, *WHO/SDE/OEH.02.2*, Geneva.
World Meteorological Organization (2007), *Scientific Assessment of Ozone Depletion: 2006, Rep. 50*, 572 pp., Geneva.
World Meteorological Organization (2011), *Scientific Assessment of Ozone Depletion: 2010, Rep. 512*, 516 pp., Geneva.